Prediction of the Magneto-Resistance of $La_{0.67}Ca_{0.33}MnO_3$ and $La_{0.8}Sr_{0.2}MnO_3$ via Temperature and a Magnetic Field

Liu Changshi*

Division of Mathematics, Physics and Information Engineering, Nan Hu Department, Jiaxing College, 118 Jia-Hang Road, Jiaxing City, Zhejiang, 314001, P. R. China

Temperature- and magnetic field-dependent resistivity is a crucial parameter in determining the physical properties of manganites. The first objective of this work was to find out an applicable method of using temperature to predict the resistivity and control the transition of $La_{0.8}Sr_{0.2}MnO_3$ and $La_{0.67}Ca_{0.33}MnO_3$ from the insulator phase to the metal phase in the transition area. Predicated on nonlinear curve fitting, a typical numerical method is used to quantitatively analyze the temperature-dependent resistivity for temperatures both less than and higher than the metal−insulator transition temperature (T_p). The simulations agree very well with the observed spectra (resistivity versus temperature). The second objective of this work was to find out the mathematical relationships between the magnetic field and the maximum resistivity ρ_{max} as well as the metal−insulator transition temperature, T_p. On the basis of the calculated results from the nonlinear curve fitting method, the magnetic field-dependent T_p and ρ_{max} are theoretically explained successfully via three functions. The minimum correlation coefficient between the actual and the calculated data is 0.994. The average relative errors between the measured and the modeled quantities do not exceed 5.86 % in all considered cases. To my knowledge, the effects of the magnetic field on the shift of both the maximum resistivity and the metal−insulator transition temperature of manganites are quantitatively discussed for the first time.

Introduction

Since the discovery of colossal magneto-resistive effects, the magnetic perovskites of the type $La_{1-x}A_xMnO_3$ (A stands for a divalent atoms: A = Ca, Sr, Ba, Pb) have attracted much attention because of the rich physics involved as well as their potential use in device applications.[1−6] Among these compounds, $La_{0.67}Ca_{0.33}MnO_3$ and $La_{0.8}Sr_{0.2}MnO_3$ are of great interest due to their high magneto-resistance at low temperatures. Electromagnetic properties, such as resistivity, ρ, the maximum resistivity, ρ_{max}, and the metal−insulator transition temperature, T_p, are of great interest in engineering processes as well as the progress of electromagnetic theories. Systematic research of those properties as a function of temperature and magnetic field can give insight into the molecular structure of mixtures, provide information on the interaction between components, and are essential for designing and testing theoretical models of mixtures. It is believed that the phase transition of manganite materials can be predicted by analyzing the resistivity or electric resistance as a function of temperature. The spectra of the temperature dependent resistivity of a manganite material indicate its metal−insulator transitions during the temperature change and the transition order at a specific temperature. Manganite materials are ferromagnetic with a Curie temperature. The transition to magnetism is accompanied by a metal−insulator transition, the manganites being nonmetallic above and metallic below the Curie temperature. The metal−insulator transition also strongly depends on the applied magnetic field, thus leading to a large "colossal" magneto-resistance near the transition temperature. Therefore, the temperature-dependent metal−insulator (MI) transition is probably the most dramatic electromagnetic property.

The most effective way to understand a physical phenomenon is to find a mathematical expression by which the quantitative relationship between two physical terms can be described. However, at present three models, that is, Arrhenius law,[7] polaron model,[8] and variable-range hopping model,[9] are used to fit high-temperature ($T > T_p$) resistivity data on the manganites, where T_p is the metal−insulator transition temperature. These three laws are very important in manganite research because they very well describe the observed high-temperature variation in the conduction mechanism. However, it has to be kept in mind that the pure Arrhenius law might be a very crude approximation.[10] The polaron model is valid only for temperatures higher than half the Debye temperature Θ_D[10]. When the carriers are localized by random potential fluctuation, Mott's variable-range hopping model is effective.[10] Although the above three laws can give an acceptable explanation for the relationship between the resistivity and the temperature in the paramagnetic phase, there is still no clear conclusion of whether or not the resistivity can be continuously predicted by temperature from the insulator phase to the metal phase for individual manganite with only one equation. The interest in resistivity and electric resistance is growing in the context of manganite. Unfortunately, few studies address this subject. Resistivity is usually one of the important physical parameters characterizing a new compound. However, accurate calculations of resistivities are quite difficult from a theoretical perspective. Hence, in this work, a mathematical function was first chosen to predict resistivity from the insulator phase to the metal phase that is as close as practically possible to $La_{0.67}Ca_{0.33}MnO_3$ and $La_{0.8}Sr_{0.2}MnO_3$ so

* Corresponding author. E-mail: liucs4976@sohu.com. Telephone: 086-0573-83643089. Fax: 086-0573-83643085.

10.1021/je100453x
Published on Web 12/21/2010

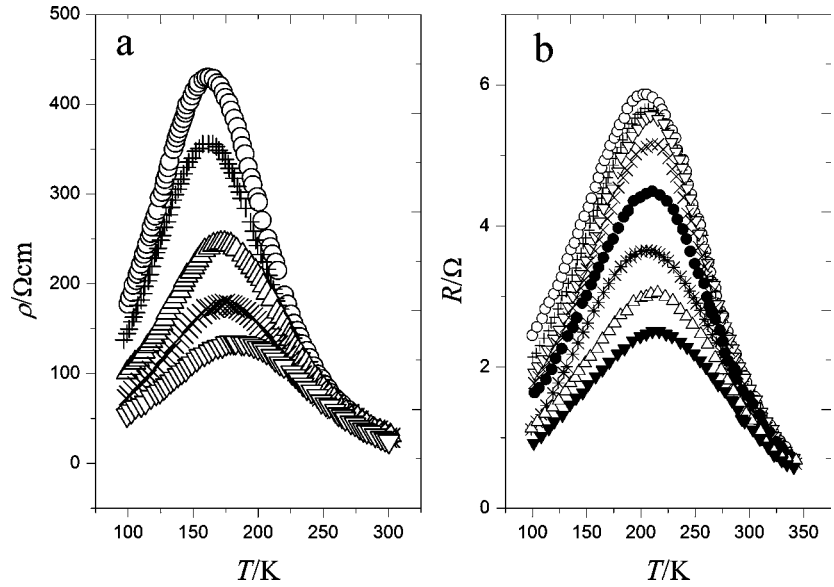

Figure 1. Resistivity, $\rho/\Omega\cdot$cm, of $La_{0.67}Ca_{0.33}MnO_3$ and electrical resistance, R/Ω, of polycrystalline $La_{0.8}Sr_{0.2}MnO_3$ as a function of absolute temperature, T, at different magnetic fields, B. In a, the resistivity, $\rho/\Omega\cdot$cm, of $La_{0.67}Ca_{0.33}MnO_3$ was applied by magnetic fields B at ○, 0 T; +, 1 T; △, 3 T; ×, 5 T; ▽, 7 T. In b, the resistance R/Ω of polycrystalline $La_{0.8}Sr_{0.2}MnO_3$ was plotted as a function of temperature, T, at magnetic fields, B, of ○, 0 T; +, 0.2 T; ▽, 0.5 T; ×, 1 T; ●, 2 T; ∗, 4 T; △, 6 T and ▼, 8 T.

that a more incisive probe on sorting out the results of the spectrum of temperature-resistivity or resistance in some cases can be provided. On the basis of the comparison between the shapes of experimental curves and the shape of the Gauss function, 13 resistivity and electric resistance curves as a function of temperature are simulated in the following sections. Second, to forecast the key electromagnetic parameters of manganites, the formula for comprehending the effects of the magnetic field on the maximum resistivity, ρ_{max}, and metal−insulator transition temperature, T_p, is proposed from data fitting of computer simulations. Satisfactory agreement is reached between the measured ρ_{max} and the modeled one. At the same time, T_p is obtained for $La_{0.67}Ca_{0.33}MnO_3$ and $La_{0.8}Sr_{0.2}MnO_3$. Therefore, the proposed approach allows estimation of the shifts of T_p and ρ_{max} for individual manganite materials.

Simulation

The resistivity of manganite materials is determined by several parameters such as composition, temperature, the applied magnetic field, grain size, and so on. Some values of resistivity and electric resistance were generated[11,12] to show the application of the method. The obtained raw data are shown in Figure 1 versus temperature. The effects of both temperature and the applied magnetic field on the resistivity of nanocrystalline $La_{0.67}Ca_{0.33}MnO_3$ are illustrated in Figure 1a[11] at low temperatures. A typical plot of variation of electrical resistance with temperature in the case of polycrystalline $La_{0.8}Sr_{0.2}MnO_3$ at different magnetic field runs is shown in Figure 1b.[12]

There is one peak in each spectrum of the 13 curves in Figure 1. The temperature dependences of the measured resistivity and electrical resistance (Figure 1) are typical for magnetoresistive materials, exhibiting a two-phase behavior with a more conductive (metallic) and a less conductive (insulating) region separated by a pronounced maximum at the peak temperature T_p. The peak temperature is also known as the metal−insulator transition temperature. This characteristic shows that resistivity or electrical resistance increases slowly in the range from 0 to T_p and drops down rapidly when the temperature is larger than T_p. Therefore, every curve is a cusp. The conduction mechanism of manganites at high temperature ($T_p < T$) has been explained by the simple Arrhenius law, the polaron model, and the variable-range hopping model law in the past.

It can be concluded that the patterns shown in Figure 1 can be analyzed in detail with fitted parameters of the desired model. The tactful way to find the mathematical relationship between the resistivity and the temperature or magnetic field is to fit the curve. There are two paths for curve fitting. One way is to directly apply the fitting function; another way is to create a mathematical model when there is no appropriate fitting function available. After checking the fitting function, it is found that the first strategy is effective enough in this work and the Gauss function offers such an opportunity. The applicable Gauss function is expressed by eq 1

$$\rho(T) = \rho(T_u) + \frac{A}{w\sqrt{\pi/2}}\exp(-2(T/\mathrm{K} - T_d/\mathrm{K})^2/w^2) \quad (1)$$

where $\rho(T_u)$, A, T_d, and w are constants and will be optimized. If the Gauss function (1) is available for predicting resistivity ρ for an individual manganite at temperatures across the measurement range, the minimum value of ρ is given by $\rho(T|_{T\to\infty})$. Hence, the physical significance of parameter $\rho(T_u)$ is the resistivity of manganite materials at very high temperatures. The maximum data of ρ are given by parameter $\rho(T_u)$, A, and w in the following form

$$\rho_{max} = \rho|_{T_u\to\infty} + \frac{A}{w\sqrt{\pi/2}} \quad (2)$$

So it is easy to rewrite the Gauss function (1) as

$$\rho(T) = \rho_{min} + \frac{A}{w\sqrt{\pi/2}}\exp(-2(T/\mathrm{K} - T_d/\mathrm{K})^2/w^2) \quad (3)$$

Table 1. Results of the Simulation of the 13 Spectra Made of Temperature *T*/K and Resistivity $\rho/\Omega\cdot$cm or Electric Resistance R/Ω[a]

materials and applied magnetic fields *B*	function form	*R* with Gauss	ARE with Gauss/%
$La_{0.67}Ca_{0.33}MnO_3$, 0 T	$\rho(T) = 40.41 + \frac{40633.2}{84.6\sqrt{\pi/2}} \exp(-2(T - 161.9)^2/84.6^2)$	0.999	3.48
$La_{0.67}Ca_{0.33}MnO_3$, 1 T	$\rho(T) = 44.29 + \frac{32093.2}{83.5\sqrt{\pi/2}} \exp(-2(T - 162.1)^2/83.5^2)$	0.998	4.30
$La_{0.67}Ca_{0.33}MnO_3$, 3 T	$\rho(T) = 32.33 + \frac{24260.0}{91.8\sqrt{\pi/2}} \exp(-2(T - 172.4)^2/91.8^2)$	0.999	2.5
$La_{0.67}Ca_{0.33}MnO_3$, 5 T	$\rho(T) = 28.75 + \frac{17725.6}{96.5\sqrt{\pi/2}} \exp(-2(T - 174.8)^2/96.5^2)$	0.999	2.3
$La_{0.67}Ca_{0.33}MnO_3$, 7 T	$\rho(T) = 16.40 + \frac{15677.8}{106.5\sqrt{\pi/2}} \exp(-2(T - 182.5)^2/106.5^2)$	0.999	1.53
$La_{0.8}Sr_{0.2}MnO_3$, 0 T	$R(T) = 0.36 + \frac{845.1}{124.7\sqrt{\pi/2}} \exp(-2(T - 197.4)^2/124.7^2)$	0.994	3.98
$La_{0.8}Sr_{0.2}MnO_3$, 0.2 T	$R(T) = 0.44 + \frac{770.}{120.8\sqrt{\pi/2}} \exp(-2(T - 201.2)^2/120.8^2)$	0.994	4.65
$La_{0.8}Sr_{0.2}MnO_3$, 0.5 T	$R(T) = 0.56 + \frac{696.6}{113.6\sqrt{\pi/2}} \exp(-2(T - 203.7)^2/113.6^2)$	0.995	5.86
$La_{0.8}Sr_{0.2}MnO_3$, 1 T	$R(T) = 0.48 + \frac{658.2}{114.1\sqrt{\pi/2}} \exp(-2(T - 204.2)^2/114.1^2)$	0.997	4.48
$La_{0.8}Sr_{0.2}MnO_3$, 2 T	$R(T) = 0.45 + \frac{598.8}{119.9\sqrt{\pi/2}} \exp(-2(T - 204.4)^2/119.9^2)$	0.996	3.48
$La_{0.8}Sr_{0.2}MnO_3$, 4 T	$R(T) = 0.26 + \frac{548.8}{129.0\sqrt{\pi/2}} \exp(-2(T - 205.7)^2/129.0^2)$	0.996	3.81
$La_{0.8}Sr_{0.2}MnO_3$, 6 T	$R(T) = 0.32 + \frac{442.8}{131.3\sqrt{\pi/2}} \exp(-2(T - 208.5)^2/131.3^2)$	0.996	3.40
$La_{0.8}Sr_{0.2}MnO_3$, 8 T	$R(T) = 0.18 + \frac{400.7}{139.1\sqrt{\pi/2}} \exp(-2(T - 210.7)^2/139.1^2)$	0.998	2.43

[a] *R*: correlation coefficient; ARE: average relative error.

This paper analyzes the resistivity curves of $La_{0.67}Ca_{0.33}MnO_3$ and electrical resistance curves of $La_{0.8}Sr_{0.2}MnO_3$ at different magnetic fields according to the above approach (3). Then through experimental raw data employed in the method of the regression analysis, the experimental spectra for $La_{0.67}Ca_{0.33}MnO_3$ and $La_{0.8}Sr_{0.2}MnO_3$ in various magnetic fields have been simulated using the component spectra shown in Figure 1. Optimized parameters employed to simulate the component spectra are also listed in Table 1. The modeled verification is also carried out by a comparison of modeled resistivity obtained by numerical integration of resistivity to measured resistivity in Figure 2.[11,12] The comparison between the results of the chosen peaks and the best-fitted value of parameter T_d by the Gauss function (3) indicates that parameter T_d corresponds to the metal−insulator transition temperature, T_p. In other words, the physical significance of parameter T_d is just the metal−insulator transition temperature T_p.

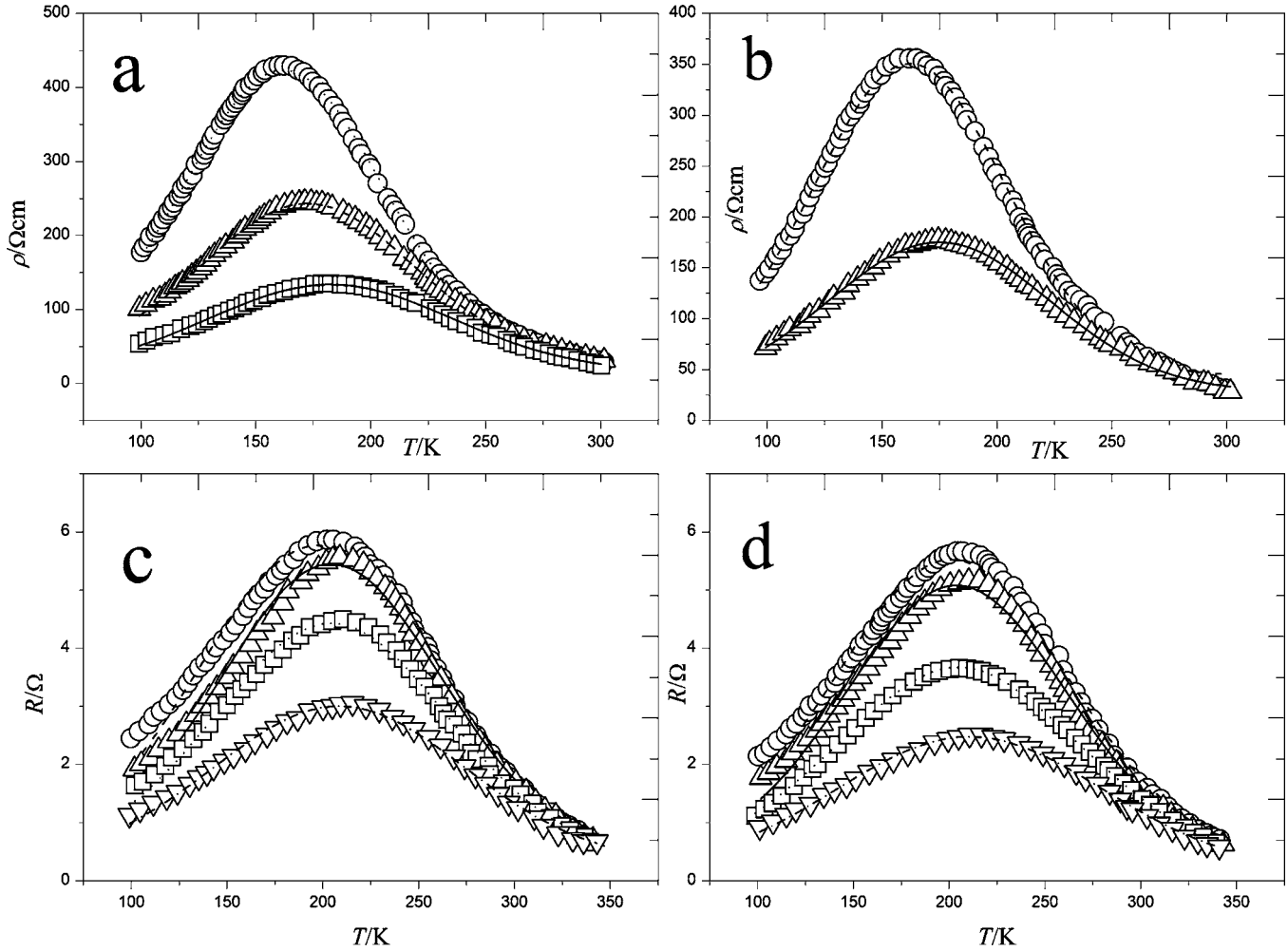

Figure 2. Comparisons between experimental and calculated temperatures, T, and the dependence of the resistivity, $\rho/\Omega\cdot$cm, for $La_{0.67}Ca_{0.33}MnO_3$ measured at several magnetic fields (a and b) as well as electrical resistance, R/Ω, for $La_{0.8}Sr_{0.2}MnO_3$ (c and d). Here, the symbols ○ and ⋯ refer to experimental and theoretical results at 0 T of magnetic field, B, in a; the symbols △ and - - - are experimental and theoretical data at 3 T of magnetic field, B, in a; the symbols □ and ─ stand for experimental and theoretical data at 7 T of magnetic field, B, in a. The symbols ○ together with - - - refer to experimental and theoretical results at 1 T of magnetic field, B, in b; the symbols △ and ─ are experimental and theoretical results at 5 T of magnetic field, B, in b. The symbols ○ and - - - are experimental and theoretical results at 0 T of magnetic field, B, in c; the symbols △ and ─ refer to experimental and theoretical results at 0.5 T of magnetic field, B, in c; the symbols □ and ⋯ stand for experimental and theoretical results at 2 T of magnetic field, B, in c; the symbols ▽ and -•- are experimental and theoretical results at 6 T of magnetic field, B, in c. The symbols ○ and - - - are experimental and theoretical results at 0.2 T of magnetic field, B, in d; the symbols △ and ─ refer to experimental and theoretical results at 1 T of magnetic field, B, in d; the symbols □ and ⋯ stand for experimental and theoretical results at 4 T of magnetic field, B, in d; the symbols ▽ and -•- are experimental and theoretical results at 8 T of magnetic field, B, in d.

To verify the accuracy of the simulation, the correlation coefficient between the measured and the simulated data is given in Table 1; the minimum magnitude of the correlation coefficient is 0.994. The average relative error (ARE)

$$\left(\frac{1}{n}\sum_{i=1}^{i=n}\frac{|\rho_{\mathrm{im}} - \rho_{\mathrm{is}}|}{\rho_{\mathrm{im}}}\cdot 100\ \%\right)$$

to evaluate the simulation results is also shown in Table 1, where ρ_{im} is measured data, and ρ_{is} stands for the value obtained by simulation. The maximum value of ARE is 4.28 %. As is shown in Table 1 and Figure 2, it can be stated that a satisfactory agreement between the measured and the modeled ρ or R is achieved by the functions given in Table 1. This good agreement implies that the metal−insulator transition temperature, T_{p}, can be confirmed more precisely by the Gauss function simulation for $La_{0.67}Ca_{0.33}MnO_3$ and $La_{0.8}Sr_{0.2}MnO_3$. Moreover, the theoretical values of the minimum and the maximum resistivity of such manganite materials can be estimated in an easier way by the Gauss function simulation because it is effective from the insulator state to the metal state.

The influence of the magnetic field on the resistivity of manganites is addressed in Figure 1, which presents $\rho(T)$ of the $La_{0.67}Ca_{0.33}MnO_3$ and $La_{0.8}Sr_{0.2}MnO_3$ in the magnetic field. The enhanced magnetic field results in a decreasing of the samples' resistivity in the transition area, showing a typical colossal magneto-resistive effect. Resistivity should be among the last quantities to be evaluated in reliable theoretical calculations, since their values rely heavily on the pattern of long-range or local spin, charge, and orbital order in a material. There is some hope to reveal the quantitative relationship between the magnetic field and the maximum value of resistivity, ρ_{max}. Figure 3a,b illustrates the results of magnetic field dependence of ρ_{max} of $La_{0.8}Sr_{0.2}MnO_3$ and $La_{0.67}Ca_{0.33}MnO_3$. The best-fitted results show that the logistic equation successfully gives a quantitative relationship between ρ_{max} and magnetic field via nonlinear curve fitting, and the logistic function is written as

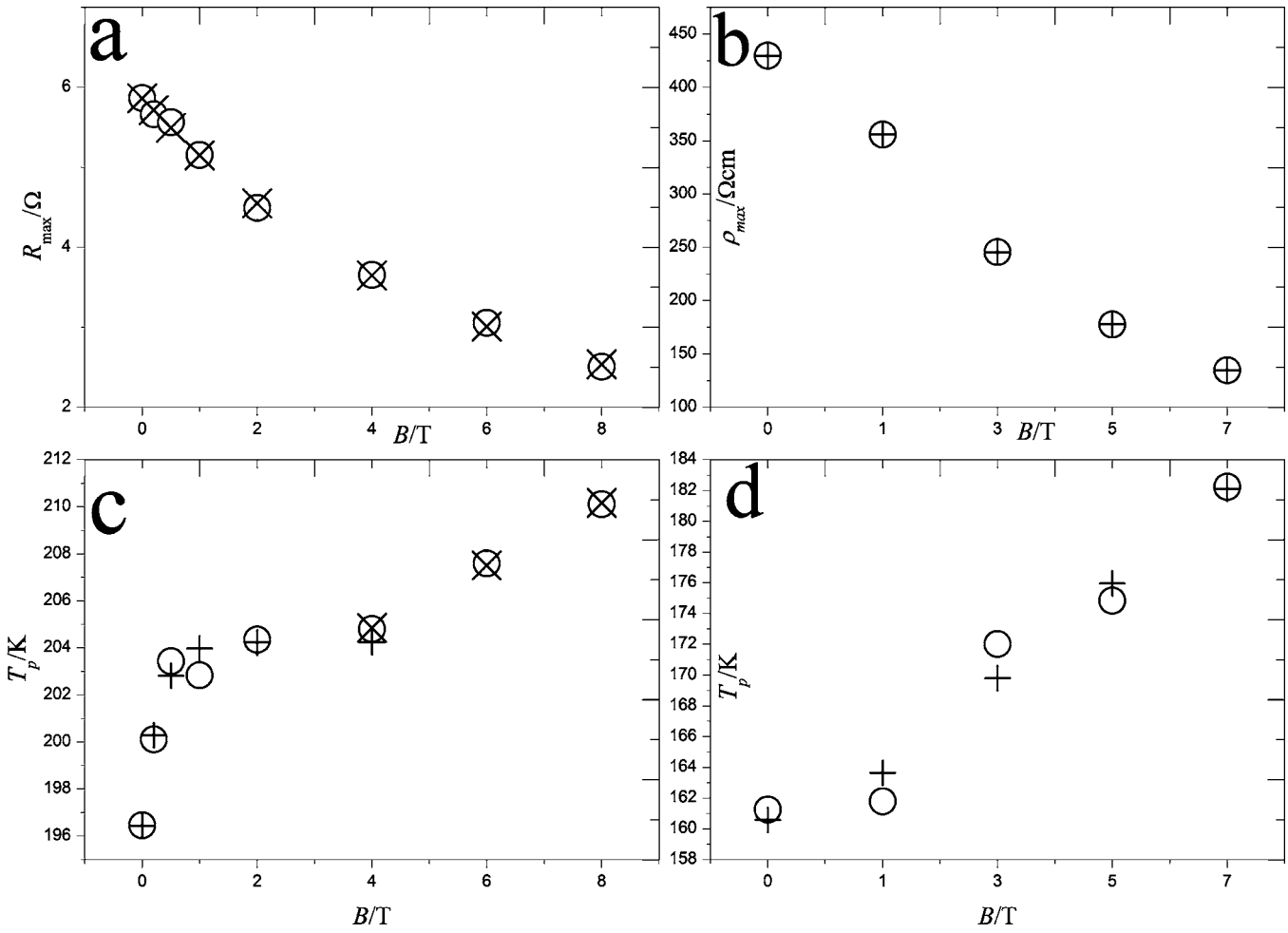

Figure 3. Geometry used to determine the maximum electrical resistance, R_{max}/Ω, of $La_{0.8}Sr_{0.2}MnO_3$, the maximum resistivity, $\rho_{max}/\Omega\cdot$cm, of $La_{0.67}Ca_{0.33}MnO_3$ and metal−insulator transition temperature, T_p, by the magnetic field, *B*. (a) Scatter plot of R_{max}/Ω against the magnetic field and least-squares curve regression. (b) Geometry used to calculate $\rho_{max}/\Omega\cdot$cm by the magnetic field. (c) Measured and modeled T_p of $La_{0.8}Sr_{0.2}MnO_3$ along the magnetic field. (d) Scatter plot of T_p of $La_{0.67}Ca_{0.33}MnO_3$ along the magnetic field and least-squares linear regression. Where the symbol ○ refers to measured data, while the symbols + together with × stand for modeled results.

$$\rho_{max}(B) = A_1 + \frac{A_1 - A_2}{1 + \left(\frac{B/T}{B_a/T}\right)^P} \quad (4)$$

In Figure 3a, the modeled R_{max} of $La_{0.8}Sr_{0.2}MnO_3$ is compared to experimental data. In the case of $La_{0.8}Sr_{0.2}MnO_3$, R_{max} as a function of the magnetic field is described as follows:

$$R_{max}(B) = 5.86 + \frac{5.86 + 0.48}{1 + \left(\frac{B/T}{7.3}\right)^{1.04}} \quad (5)$$

Using eq 5, it is found that the correlative coefficient between the fitted value of R_{max} and the measured data of R_{max} is 1.0, and the average relative error is 0.1 %.

The plots of ρ_{max} versus magnetic field for $La_{0.67}Ca_{0.33}MnO_3$ have been fitted with the logistic model, as shown in Figure 3b. The optimized parameters of A_1, A_2, and B_a obtained from the fitting of the experimental data are given by

$$\rho_{max}(B) = 429.7 + \frac{429.7 + 39.9}{1 + \left(\frac{B/T}{4.4}\right)^{1.13}} \quad (6)$$

The logistic function (eq 6) yields 1.0 for the correlative coefficient between the fitted value of ρ_{max} and the measured data of ρ_{max}, and the average relative error is 0.1 %.

Since no comprehensive theory which could explain all of the complexity of colossal magneto-resistive like phenomena has been suggested so far, the competition between CO (charge-ordering) and ferromagnetic is indeed a key component of the current theories of manganites aiming to explain the colossal magneto-resistive phenomenon. The logistic model successfully retraces the experimental behavior of the maximum resistivity in $La_{0.67}Ca_{0.33}MnO_3$ and $La_{0.8}Sr_{0.2}MnO_3$. The maximum resistivity is found to decrease with the increased magnetic field in the form of the logistic function, which implies a logistic increase in the carrier density. Hence, it is appropriate to use the logistic model in forecasting the maximum resistivity before one magnetic field is applied. Another benefit of eq 4 may be obtained by the design of magnetic field sensors.

Having discussed the mathematical relationship between magnetic field and ρ_{max}, attention should be paid to the influence of the magnetic field on the metal−insulator transition temperature, T_p. It can be seen from Figure 1 that the T_p of both $La_{0.67}Ca_{0.33}MnO_3$ and $La_{0.8}Sr_{0.2}MnO_3$ shifts toward higher temperature with increasing magnetic field. The detailed analysis inferred that T_p has some relation with magnetic field *B* (unit is T). To calculate T_p from the magnetic field, the T_p of

$La_{0.8}Sr_{0.2}MnO_3$ as a function of magnetic field B is plotted in Figure 3c. The nonlinear curve fitting is the best method of obtaining the relationship between T_p and magnetic field. In Figure 3c, the measured and modeled T_p versus magnetic field are depicted for determining T_p of $La_{0.8}Sr_{0.2}MnO_3$ using magnetic field data. The equation to characterize this relationship is written as follows:

$$T_p(B) = \begin{cases} 204.24 - 7.8\cdot(3.3\cdot 10^{-2})^{B/T}[0, 4T] \\ 199.54 + 1.33\cdot B/T[4, 8T] \end{cases} \quad (7)$$

Although the magnetic field dependence of T_p is complex in Figure 3c, the T_p data [0, 4T] of $La_{0.8}Sr_{0.2}MnO_3$ of the present investigation are found to fit well with the asymptotical function

$$T_p(B) = 204.24 - 7.8\cdot(3.3\cdot 10^{-2})^{B/T}[0, 4T] \quad (8)$$

The correlative coefficient between the fitted value of T_p in the range from (0 to 4) T and the measured data of T_p is 0.979, and the mean relative error is 0.22 %. The mathematical mechanism of T_p at high magnetic field [4, 8 T] is explained by a line equation, and the equation is given by

$$T_p(B) = 199.54 + 1.33\cdot B/T[4, 8T] \quad (9)$$

In this case, the correlative coefficient between the fitted value of T_p in the range from (4 to 8) T and the measured data of T_p is 1, and the mean relative error is 0.029 %. The asymptotical function consistently explains the relation between magnetic field and T_p in the range from (0 to 4) T for $La_{0.8}Sr_{0.2}MnO_3$. This may be due to the fact that delocalization of charge carriers are induced by the applied magnetic field very rapidly in a low field, which in turn might suppress the resistivity and also cause local ordering of the magnetic spins at the same speed. Because of this ordering, the ferromagnetic metallic state may suppress the paramagnetic insulating (PMI) regime. As a result, the conduction electrons (e_g^1) are completely polarized inside the magnetic domains and are easily transferred between the pairs of Mn^{3+} ($t_{2g}^3e_g^1$: $S = 2$) and Mn^{4+} ($t_{2g}^3e_g^{01}$: $S = 3/2$) via oxygen, and hence the peak temperature (T_p) shifts to the high-temperature side with applications of the magnetic field. In the higher field region from (4 to 8) T, delocalization of charge carriers is uniformly induced by the applied magnetic field, which in turn might suppress the resistivity and also cause local ordering of the magnetic spins in the same way.

Figure 3d shows the construct of the T_p of $La_{0.67}Ca_{0.33}MnO_3$ as the function of magnetic field. According to the regression lines for T_p and magnetic field in Figure 3d, it can be seen that there is a very simple linear relationship between the two variables. Therefore, the functional form between T_p and magnetic field for $La_{0.67}Ca_{0.33}MnO_3$ is expressed by eq 10 as follows:

$$T_p(B) = 160.57 + 3.08\cdot B/T \quad (10)$$

The correlative coefficient between the fitted value of T_p and the measured data of T_p is 0.994, and the mean relative error is 0.713 %. It is inferred from eq 10 that the applied magnetic field homogenously induces delocalization of charge carriers, which in turn might even suppress the resistivity and also uniformly cause local ordering of the magnetic spins. Due to this linear ordering, the ferromagnetic metallic state may suppress the paramagnetic insulating (PMI) regime. As a result, the conduction electrons (e_g^1) are completely polarized inside the magnetic domains and are easily transferred between the pairs of Mn^{3+} ($t_{2g}^3e_g^1$: $S = 2$) and Mn^{4+} ($t_{2g}^3e_g^{01}$: $S = 3/2$) via oxygen, and hence the peak temperature (T_p) shifts at uniform velocity to the high-temperature side with application of the magnetic field.

Impressively, it can be observed that the theoretical results of T_p derived by both eqs 7 and 10 are consistent with the experimental data in Table 1. From this it may be stated that the magnetic field is correlative with T_p. Therefore, it is feasible that eqs 7 and 10 are used to determine the change of T_p through the magnetic field. It is also appropriate to use eqs 7 and 10 in forecasting T_p before one magnetic field is applied. The direction of design for temperature-sensitive sensors may be instructed through eqs 7 and 10.

Conclusions

In this research, the resistivity of $La_{0.67}Ca_{0.33}MnO_3$ and electrical resistance of $La_{0.8}Sr_{0.2}MnO_3$ were calculated for the continuous phase transition as a function of temperature from the ferromagnetic state to the paramagnetic state. A typical mathematical function was applied. Not only can the function describe the change of the resistivity or electrical resistance with temperature across the measured range, but also it predicts some characteristic indexes of manganite materials. The theoretical values simulated in this paper are consistent with experimental data; the maximum data of mean relative errors is 5.86 %, and the minimum value of the correlation coefficient between the actual and the calculated data is 0.994. The good agreement between the measured and the simulated results of resistivity and electrical resistance indicates that the cusp peak function can accurately predict some aspects of $La_{0.67}Ca_{0.33}MnO_3$ and $La_{0.8}Sr_{0.2}MnO_3$. It is not sure that each spectrum in the form of electrical resistance or resistivity versus temperature for manganites can be simulated from the insulator phase to the metal phase, but it is true that the resistivity of $La_{0.67}Ca_{0.33}MnO_3$ and electrical resistance of $La_{0.8}Sr_{0.2}MnO_3$ can be accurately calculated because of individual differences. Since the Gauss function denotes a relaxation process, the fact that the resistivity of $La_{0.67}Ca_{0.33}MnO_3$ and electrical resistance of $La_{0.8}Sr_{0.2}MnO_3$ were fitted well with the Gauss function suggests that resistivity and electrical resistance versus absolute temperature of $La_{0.67}Ca_{0.33}MnO_3$ and $La_{0.8}Sr_{0.2}MnO_3$ is the relaxation process of Gauss. It is also worth noting that the benefit of the mathematical relationship between the magnetic field and the maximum resistivity along with the metal−insulator transition temperature reported in this paper indicates that there is not only some quantitative bridge to link the maximum resistivity and magnetic field but also some possible connection between the magnetic field and the metal−insulator transition temperature for other manganites. More importantly, the good agreement between the observed and the predicted results of magnetoresistance is helpful to understand the properties of manganites using a mathematical method.

Literature Cited

(1) Alivisatos, A. P. Semiconductor Clusters, Nanocrystals, and Quantum Dots. *Science* **1996**, *271*, 933–937.
(2) Prinz, G. A. Magnetoelectronics. *Science* **1998**, *282*, 1660–1663.
(3) Zhu, T.; Shen, B. G.; Sun, J. R.; Zhao, H. W.; Zhan, W. S. Surface spin-glass behavior in $La_{2/3}Sr_{1/3}MnO_3$ nanoparticles. *Appl. Phys. Lett.* **2001**, *78*, 3863–3866.

(4) Fu, Y. Magnetism and superconductivity-grain-boundary effects on the electrical resistivity and the ferromagnetic transition temperature of $La_{0.8}Ca_{0.2}MnO$. *Appl. Phys. Lett.* **2000**, *77*, 118–120.

(5) Venkataiah, G.; Reddy, P. V. Electrical behavior of sol-gel prepared $Nd_{0.67}Sr_{0.33}MnO_3$ Manganite system. *J. Magn. Magn. Mater*. **2005**, *285*, 343–352.

(6) Venkataiah, G.; Lakshmi, Y. K.; Prasad, V.; Reddy, V. P. Influence of Particle Size on Electrical Transport Properties of $La_{0.67}Sr_{0.33}MnO_3$ Manganite System. *J. Nanosci. Nanotechnol.* **2007**, *7*, 2000–2004.

(7) Kusters, R. M.; Singleton, J.; Keen, D. A.; McGreevy, R.; Hayes, W. Magnetoresistance measurements on the magnetic semiconductor $Nd_{0.5}Pb_{0.5}MnO_3$. *Physica B* **1989**, *155*, 362–365.

(8) Snyder, G. J.; Hiskes, R.; DiCarolis, S.; Beasley, M. R.; Geballe, T. H. Intrinsic Electrical Transport and Magnetic Properties of $La_{.67}Ca_{.33}MnO_3$ and $La_{.67}Sr_{.33}MnO_3$: A Study of Thin Films Grown Epitaxially by MOCVD. *Phys. Rev. B* **1996**, *53*, 14434–14440.

(9) Viret, M.; Ranno, L.; Coey, J. M. D. Magnetic localization in mixed-valence manganites. *Phys. Rev. B* **1997**, *55*, 8067–8070.

(10) Ziese, M.; Srinitiwarawong, C. Polaronic effects on the resistivity of Manganite thin films. *Phys. Rev. B* **1998**, *58*, 11519–11525.

(11) Venkataiah, G.; Lakshmi, Y. K.; Reddy, P. V. Influence of sintering temperature on resistivity, magnetoresistance and thermopower of $La_{0.67}Ca_{0.33}MnO_3$. *PMC Phys. B* **2008**, *1*, 1–12.

(12) Sergeenkov, S.; Mucha, J.; Pekala, M.; Drozd, V.; Ausloos, M. Influence of Zeeman splitting and thermally excited polaron states on magnetoelectrical and magnetothermal properties of magnetoresistive polycrystalline Manganite $La_{0.8}Sr_{0.2}MnO_3$. *J. Appl. Phys.* **2007**, *102*, 083916-1−083916-9.

Received for review May 2, 2010. Accepted December 3, 2010.

JE100453X